

Online Palmprint Identification

David Zhang, *Senior Member, IEEE*, Wai-Kin Kong, *Member, IEEE*,
Jane You, *Member, IEEE*, and Michael Wong

Abstract—Biometrics-based personal identification is regarded as an effective method for automatically recognizing, with a high confidence, a person's identity. This paper presents a new biometric approach to online personal identification using palmprint technology. In contrast to the existing methods, our online palmprint identification system employs low-resolution palmprint images to achieve effective personal identification. The system consists of two parts: a novel device for online palmprint image acquisition and an efficient algorithm for fast palmprint recognition. A robust image coordinate system is defined to facilitate image alignment for feature extraction. In addition, a 2D Gabor phase encoding scheme is proposed for palmprint feature extraction and representation. The experimental results demonstrate the feasibility of the proposed system.

Index Terms—Biometrics, online palmprint identification, texture analysis, low-resolution image.

1 INTRODUCTION

THE rapid growth in the use of *e-commerce* applications requires reliable and automatic personal identification for effective security control. Traditional, automatic, personal identification can be divided into two categories: token-based, such as a physical key, an ID card, and a passport, and knowledge-based, such as a password. However, these approaches have some limitations. In the token-based approach, the "token" can be easily stolen or lost. In the knowledge-based approach, to some extent, the "knowledge" can be guessed or forgotten. Thus, biometric personal identification is emerging as a powerful means for automatically recognizing a person's identity. The biometric computing-based approach is concerned with identifying a person by his/her physiological characteristics, such as iris pattern, retina, palmprint, fingerprint, and face, or using some aspect of his/her behavior, such as voice, signature, and gesture [1], [2]. Fingerprint-based personal identification has drawn considerable attention over the last 25 years [17]. However, workers and elderly may not provide clear fingerprint because of their problematic skins and physical work. Recently, voice, face, and iris-based verifications have been studied extensively [1], [2], [12], [13], [14], [15], [16]. As a result, many biometric systems for commercial applications have been successfully developed. Nevertheless, limited work has been reported on palmprint identification and verification, despite the importance of palmprint features.

There are many unique features in a palmprint image that can be used for personal identification. Principal lines, wrinkles, ridges, minutiae points, singular points, and

texture are regarded as useful features for palmprint representation [6]. Various features can be extracted at different image resolutions. For features such as minutiae points, ridges, and singular points, a high-resolution image, with at least 400 dpi (dots per inch), is required for feature extraction [7]. However, features like principal lines and wrinkles, which are defined in Fig. 1, can be obtained from a low-resolution palmprint image with less than 100 dpi [3], [6]. In general, high-resolution images are essential for some applications such as law enforcement, where ridges, singular points, and minutiae points are extracted and matched in latent prints for identification and verification. Some companies, including NEC and PRINTRAK, have developed automatic palmprint identification and verification systems for law enforcement applications [8], [20]. For civil and commercial applications, low-resolution palmprint images are more suitable than high-resolution images because of their smaller file sizes, which results in shorter computation times during preprocessing and feature extraction. Therefore, they are useful for many real-time palmprint applications.

Automatic palmprint identification systems can be classified into two categories: *online* and *offline*. An online system captures palmprint images using a palmprint capture sensor that is directly connected to a computer for real-time processing. An offline palmprint identification system usually processes previously captured palmprint images, which are often obtained from inked palmprints that were digitized by a digital scanner. In the past few years, some researchers have worked on offline palmprint images and have obtained useful results [3], [4], [5], [6], [7], [9]. Recently, several researchers have started to work on online palmprint images that are captured by CCD (charge-coupled device) cameras or digital scanners [18], [19]. In contrast to the existing online approaches, we develop an online palmprint identification system for civil and commercial applications, that uses low-resolution images.

There are three key issues to be considered in developing an online palmprint identification system:

1. Palmprint Acquisition: How do we obtain a good quality palmprint image in a short time interval,

- The authors are with the Department of Computing, The Hong Kong Polytechnic University, Hung Hom, Hong Kong.
E-mail: {csdzhang, csuokong, csyjia, csmkwong}@comp.polyu.edu.hk.
- D. Zhang is also with the Biometrics Research Centre, Department of Computing, The Hong Kong Polytechnic University, Hung Hom, Kowloon, Hong Kong.

Manuscript received 3 June 2002; revised 27 Nov. 2002; accepted 17 Feb. 2003.

Recommended for acceptance by K. Yamamoto.

For information on obtaining reprints of this article, please send e-mail to: tpami@computer.org, and reference IEEECS Log Number 116673.

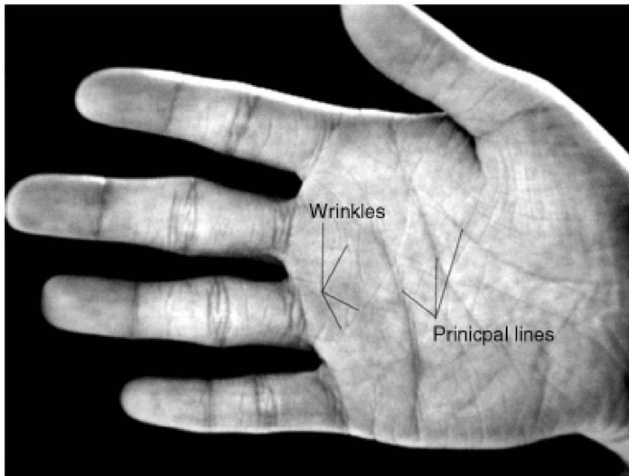


Fig. 1. Palmprint feature definitions with principal lines and wrinkles.

such as 1 second? What kind of device is suitable for data acquisition?

2. Palmprint Feature Representation: Which types of palmprint features are suitable for identification? How to represent different palmprint features?
3. Palmprint Identification: How do we search for a queried palmprint in a given database and obtain a response within a limited time?

So far, several companies have developed special scanners to capture high-resolution palmprint images [8], [20]. These devices can extract many detailed features, including minutiae points and singular points, for special applications. Although these platform scanners can meet the requirements of online systems, they are difficult to use in real-time applications because a few seconds are needed to scan a palm. To achieve online palmprint identification in real-time, a special device is required for fast palmprint sampling. Previously, our research team has successfully developed a CCD camera based on a special device for online palmprint acquisition. A brief description of this special device is presented in Section 2.1.

Palmprint feature representation depends on image resolution. In high-resolution palmprint images (> 400 dpi), many features that are similar to singular points and minutiae points in a fingerprint can be obtained; however, these features cannot be observed in low-resolution images (< 100 dpi). Nevertheless, we can extract principal lines and wrinkles from low-resolution images. In fact, line features play an important role in palmprint identification [3], [4]. Unfortunately, it is difficult to obtain a high recognition rate using only principal lines because of their similarity among different people. It is noted that texture representation for coarse-level palmprint classification provides an effective approach [5]. In this paper, we explore the use of texture to represent low-resolution palmprint images for online personal identification.

The rest of this paper is organized as follows: Section 2 gives a brief description of our low-resolution-based, online palmprint identification system. A palmprint coding scheme and palmprint matching using hamming distance are detailed in Section 3. Section 4 reports our experimental results for both identification and verification. Finally, the conclusion and future work are presented in Section 5.

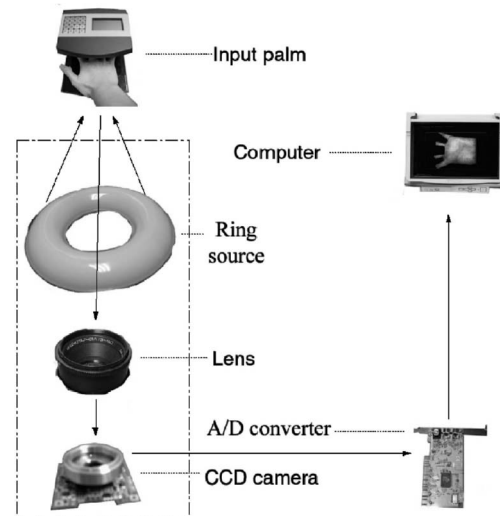


Fig. 2. The design principle of the palmprint capture device.

2 SYSTEM DESCRIPTION

In this paper, we utilize palmprint images with 75 dpi resolution to develop a real-time palmprint identification system that consists of two parts: a novel device for online palmprint image acquisition, and an effective algorithm for fast palmprint recognition.

2.1 Online Palmprint Image Acquisition

Our palmprint capture device includes ring source, CCD camera, lens, frame grabber, and A/D (analogue-to-digital)

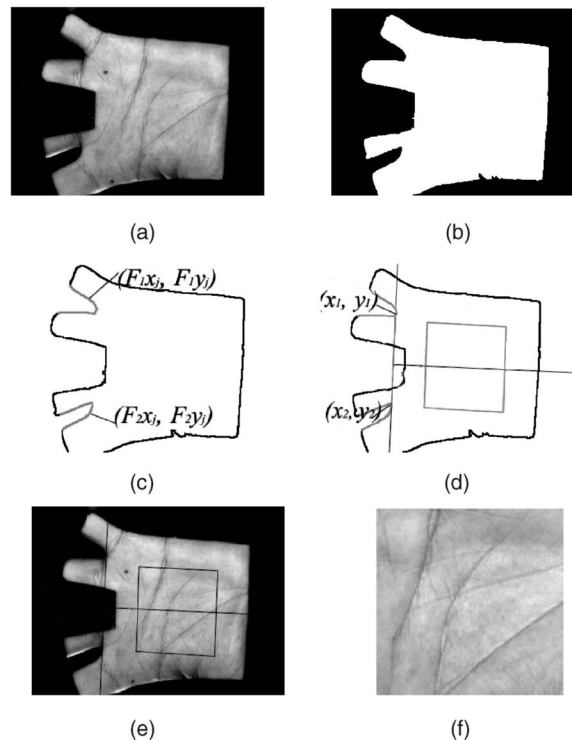


Fig. 3. The main steps of preprocessing. (a) Original image, (b) binary image, (c) boundary tracking, (d) building a coordinate system, (e) extracting the central part as a subimage, and (f) preprocessed result.

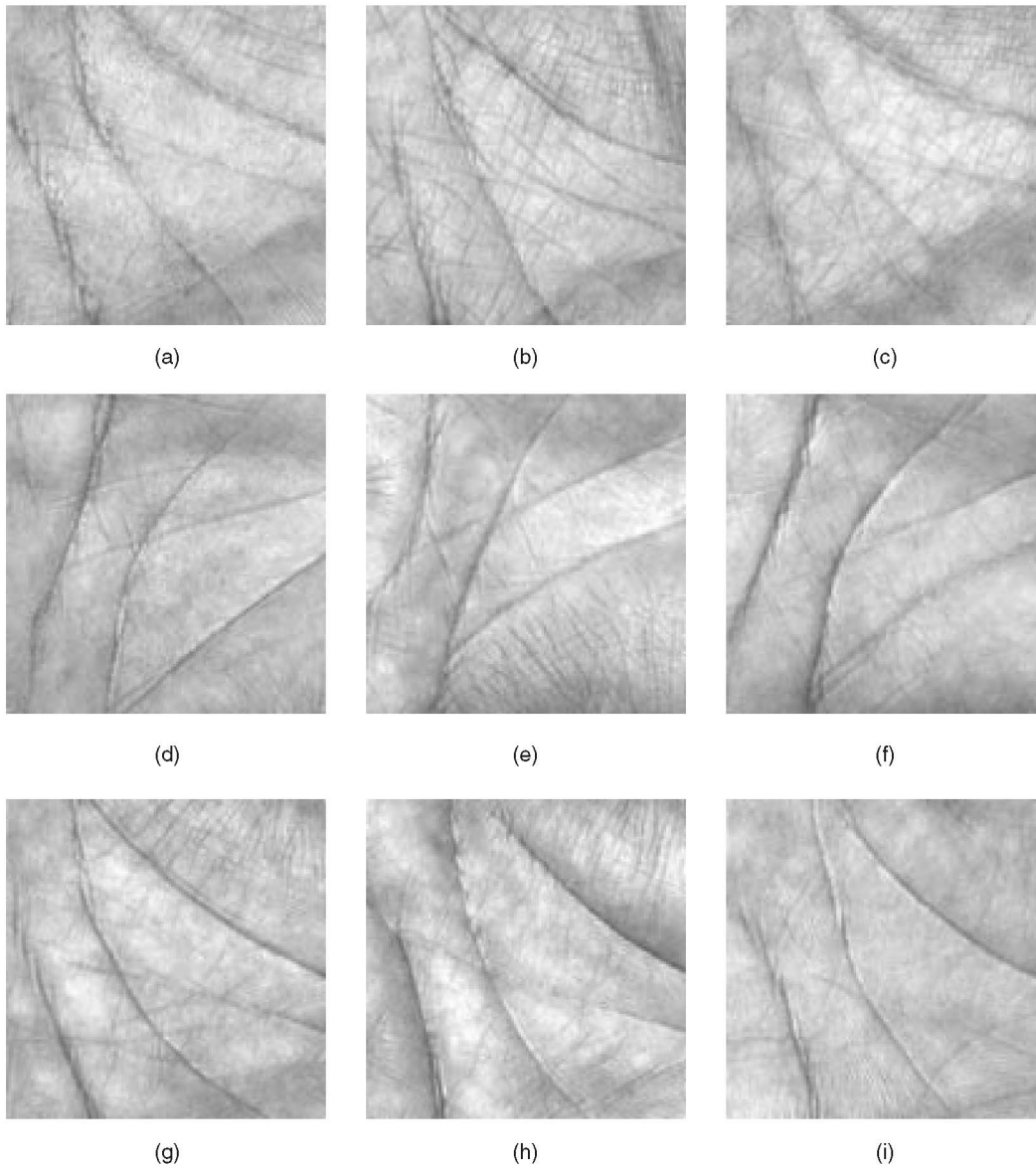


Fig. 4. The sets of the palmprint images with the similar principal lines.

converter. To obtain a stable palmprint image, a case and a cover are used to form a semiclosed environment, and the ring source provides uniform lighting conditions during palmprint image capturing. Also, six pegs on the platform serve as control points for the placement of the user's hands. The A/D converter directly transmits the images captured by the CCD camera to a computer. Fig. 2 shows a schematic diagram of our online palmprint capture device. Palmprint images can be obtained in two different sizes, 384×284 and 768×568 .

2.2 Coordinate System: Preprocessing

It is important to define a coordinate system that is used to align different palmprint images for matching. To extract the central part of a palmprint, for reliable feature measurements, we use the gaps between the fingers as reference points to determine a coordinate system. The five major steps (see Fig. 3) in processing the image are:

Step 1. Apply a lowpass filter, $L(u, v)$, such as Gaussian smoothing, to the original image, $O(x, y)$. A threshold, T_p , is used to convert the convolved image to a binary image, $B(x, y)$, as shown in Fig. 3b.

Step 2. Obtain the boundaries of the gaps, $(F_i x_j, F_i y_j)$ ($i = 1, 2$), between the fingers using a boundary tracking algorithm (see Fig. 3c). The boundary of the gap between the ring and middle fingers is not extracted since it is not useful for the following processing.

Step 3. Compute the tangent of the two gaps. Let (x_1, y_1) and (x_2, y_2) be any points on $(F_1 x_j, F_1 y_j)$ and $(F_2 x_j, F_2 y_j)$, respectively. If the line $(y = mx + c)$ passing through these two points satisfies the inequality, $F_i y_j \leq m F_i x_j + c$, for all i and j (see Fig. 3d), then the line $(y = mx + c)$ is considered to be the tangent of the two gaps.

Step 4. Line up (x_1, y_1) and (x_2, y_2) to get the Y-axis of the palmprint coordinate system, and use a line passing through the midpoint of these two points, which is

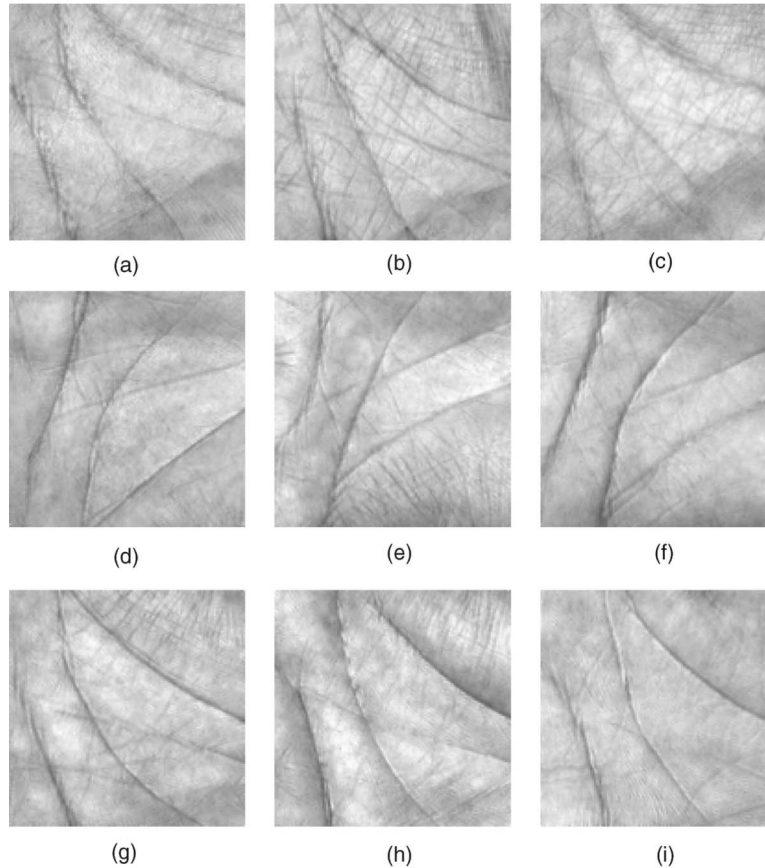


Fig. 5. Typical preprocessed palmprint images without clear wrinkles.

perpendicular to the Y-axis, to determine the origin of the coordinate system (see Fig. 3d).

Step 5. Extract a subimage of a fixed size based on the coordinate system. The subimage is located at a certain area of the palmprint image for feature extraction (see Figs. 3e and 3f).

3 PALMPRINT REPRESENTATION AND IDENTIFICATION

3.1 Feature Extraction and Coding

As mentioned before, a palmprint can be represented by some line features from a low-resolution image. Algorithms such as the stack filter [9] are able to extract the principal lines. However, these principal lines are not sufficient to represent the uniqueness of each individual's palmprint because different people may have similar principal lines in their palmprints. Fig. 4 demonstrates this problem by showing nine different palmprint samples that have similar principal lines. In addition, some palmprint images do not have clear wrinkles (see Fig. 5). As a result, we try to extract texture features from low-resolution palmprint images, and we propose a 2D Gabor phase coding scheme for palmprint representation, which has been used for iris recognition [12].

The circular Gabor filter is an effective tool for texture analysis [12], and has the following general form:

$$G(x, y, \theta, u, \sigma) = \frac{1}{2\pi\sigma^2} \exp\left\{-\frac{x^2 + y^2}{2\sigma^2}\right\} \exp\{2\pi i(ux \cos \theta + uy \sin \theta)\}, \quad (1)$$

where $i = \sqrt{-1}$, u is the frequency of the sinusoidal wave, θ controls the orientation of the function, and σ is the standard deviation of the Gaussian envelope. To make it more robust against brightness, a discrete Gabor filter, $G[x, y, \theta, u, \sigma]$, is turned to zero DC (direct current) with the application of the following formula:

$$\tilde{G}[s, y, \theta, u, \sigma] = G[x, y, \theta, u, \sigma] - \frac{\sum_{i=-n}^n \sum_{j=-n}^n G[i, j, \theta, u, \sigma]}{(2n+1)^2}, \quad (2)$$

where $(2n+1)^2$ is the size of the filter. In fact, the imaginary part of the Gabor filter automatically has zero DC because of odd symmetry. The adjusted Gabor filter is used to filter the preprocessed images.

It should be pointed out that the success of 2D Gabor phase coding depends on the selection of Gabor filter parameters, θ , σ , and u . In our system, we applied a tuning process to optimize the selection of these three parameters. As a result, one Gabor filter with optimized parameters, $\theta = \pi/4$, $u = 0.0916$, and $\sigma = 5.6179$ is exploited to generate a feature vector with 2,048 dimensions. In addition, we also include an automatic *thresholding* procedure to handle the misplacement of the palm during data sampling. In some cases, a user does not place his/her hand correctly and some *nonpalmprint pixels* will be included in the preprocessed images. A typical

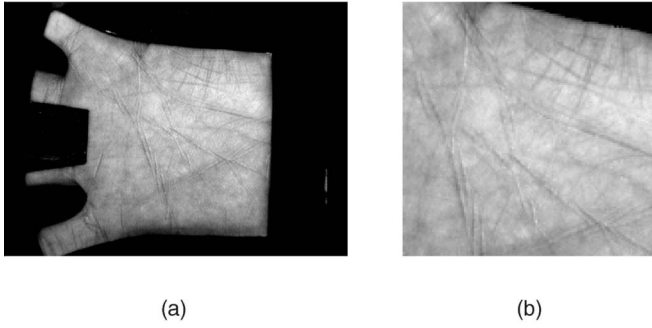


Fig. 6. (a) Incorrect placement of a palm and (b) the corresponding preprocessed image.

example is shown in Fig. 6, which shows the incorrect placement of a user's palm and the corresponding preprocessed palmprint image containing a redundant black region. To remove such redundant information from the image, we generate a mask to identify the location of the nonpalmprint pixels. Based on the semiclosed environment of the scanning device, the nonpalmprint pixels are mainly caused by the black boundaries of the platform. Thus, we can easily use a threshold to segment these nonpalmprint pixels. Fig. 7

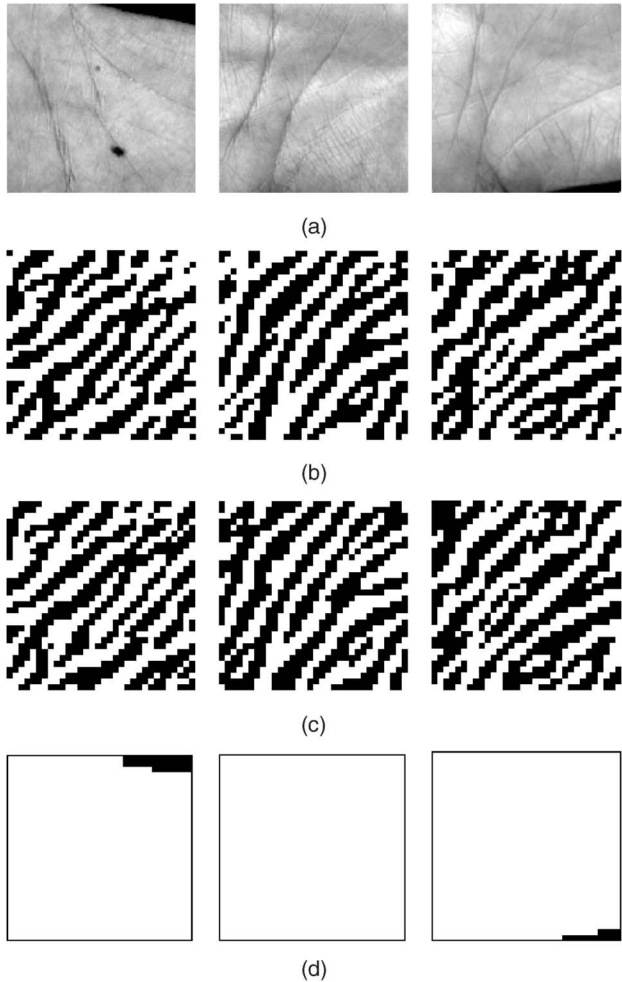


Fig. 7. Feature features obtained by 2D Gabor filtering. (a) Preprocessed images, (b) real parts of texture images, (c) imaginary parts of texture features, and (d) the corresponding masks.

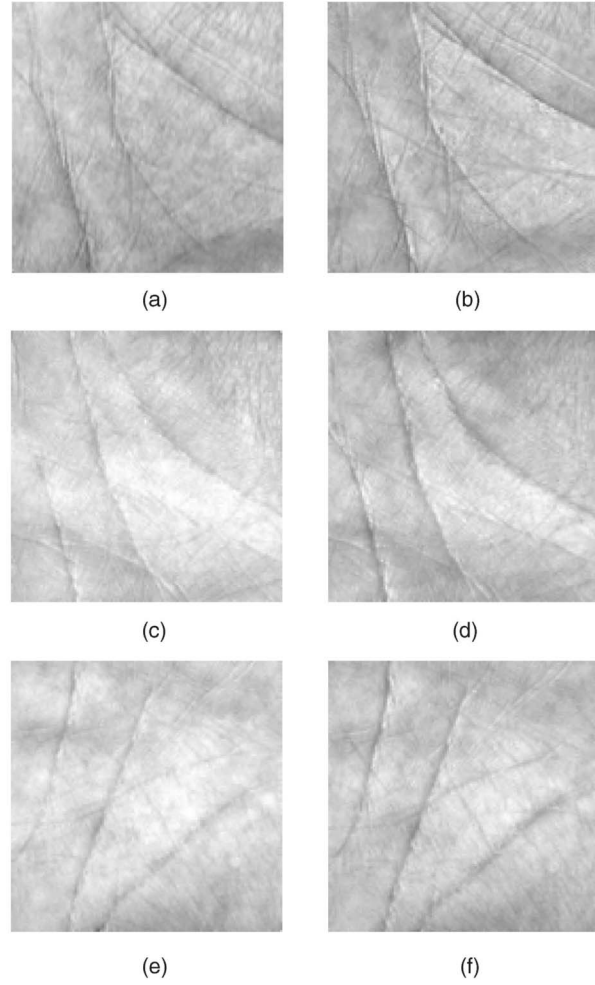


Fig. 8. The palmprint images captured at the different time from the same person. (a), (c), and (e) first collected images, and (b), (d), and (f) second collected images.

depicts the preprocessed images, showing the texture features obtained after 2D Gabor filtering and the corresponding masks.

3.2 Palmprint Matching

Given two data sets, a matching algorithm determines the degree of similarity between them. To describe the matching process clearly, we use a feature vector to represent image data that consists of two feature matrices, real and imaginary. A normalized Hamming distance used in [12] is adopted to determine the similarity measurement for palmprint matching. Let P and Q be two palmprint feature vectors. The normalized hamming distance can be described as

$$D_o = \frac{\sum_{i=1}^N \sum_{j=1}^N P_M(i,j) \cap Q_M(i,j) \cap (P_R(i,j) \otimes Q_R(i,j)) + P_M(i,j) \cap Q_M(i,j) \cap (P_I(i,j) \otimes Q_I(i,j))}{2 \sum_{i=1}^N \sum_{j=1}^N P_M(i,j) \cap Q_M(i,j)}, \quad (3)$$

TABLE 1
The Matching Scores among the Images in
(a) Fig. 4, (b) Fig. 8, and (c) Fig. 9

Figs	4(b)	4(c)	4(d)	4(e)	4(f)	4(g)	4(h)	4(i)
4(a)	0.44	0.47	0.43	0.43	0.47	0.46	0.44	0.44
4(b)		0.45	0.45	0.44	0.45	0.43	0.42	0.45
4(c)			0.39	0.48	0.39	0.39	0.44	0.48
4(d)				0.39	0.36	0.42	0.45	0.43
4(e)					0.42	0.41	0.45	0.42
4(f)						0.39	0.46	0.44
4(g)							0.45	0.45
4(h)								0.43

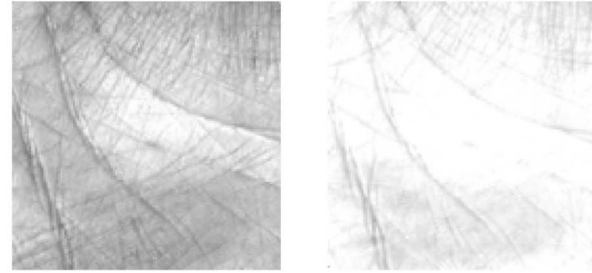
(a)

Figs	8(b)	8(c)	8(d)	8(e)	8(f)
8(a)	0.31	0.41	0.42	0.46	0.46
8(b)		0.43	0.42	0.46	0.46
8(c)			0.27	0.44	0.45
8(d)				0.42	0.42
8(e)					0.23

(b)

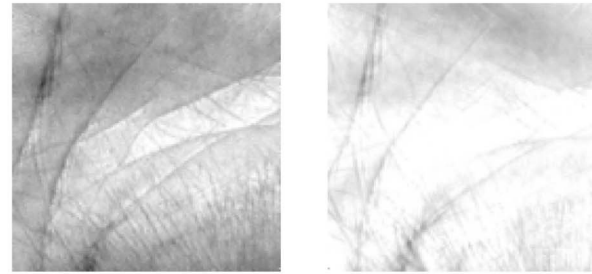
Figs	9(b)	9(c)	9(d)	9(e)	9(f)
9(a)	0.26	0.41	0.39	0.46	0.44
9(b)		0.42	0.4	0.45	0.45
9(c)			0.31	0.43	0.43
9(d)				0.43	0.46
9(e)					0.26

(c)



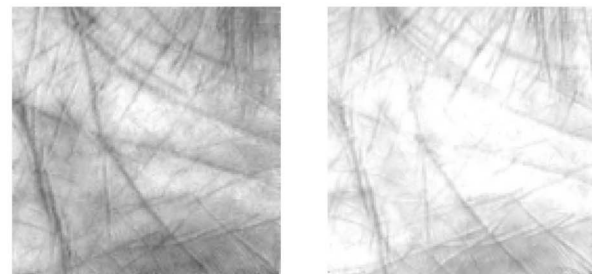
(a)

(b)



(c)

(d)



(e)

(f)

where $P_R(Q_R)$, $P_I(Q_I)$, and $P_M(Q_M)$ are the real part, the imaginary part and the mask of $P(Q)$, respectively. The result of the Boolean operator (\otimes) is equal to zero if and only if the two bits, $P_{R(I)}(i, j)$, are equal to $Q_{R(I)}(i, j)$; the symbol \cup represents the AND operator, and the size of the feature matrixes is $N \times N$. It is noted that D_o is between 1 and 0. For the best matching, the hamming distance should be zero. Because of imperfect preprocessing, we need to vertically and horizontally translate one of the features and match again. The ranges of the vertical and horizontal translations are defined from -2 to 2 . The minimum D_0 value obtained from the translated matchings is considered to be the final matching score.

4 EXPERIMENTAL RESULTS

4.1 Palmprint Database

We collected palmprint images from 193 individuals using our palmprint capture device. The subjects mainly consisted of volunteers from the students and staff at the Hong Kong Polytechnic University. In this dataset, 131 people are male, and the age distribution of the subjects is: younger than 30 years old is about 86 percent, older than 50 is about 3 percent, with about 11 percent aged between 30 and 50. In addition, we collected the palmprint images on two separate occasions, at an interval of around two months. On each occasion, the subject was asked to provide about 10 images, each of the left palm and the right palm. We also

gave some instructions to the subjects for using our capture device. Therefore, each person provided around 40 images, so that our database contained a total of 7,752 images from 386 different palms. In addition, we changed the light source and adjusted the focus of the CCD camera so that the images collected on the first and second occasions could be regarded as being captured by two different palmprint devices. The average time interval between the first and second occasions was 69 days. The maximum and minimum time intervals were 162 days and 4 days, respectively. Originally, the collected images were of two different sizes, 384×284 and 768×568 . The larger image was resized to 384×284 . Consequently, the size of all the test images used in the following experiments was 384×284 with 75 dpi resolution. Fig. 8 shows three sets of preprocessed palmprint images that were captured at two different occasions. Their matching scores are shown in Table 1b. Note that the Hamming distances between two palmprint images from the same hand differ by, at most, 0.31. As a comparison, in the nine images that have similar principal lines from different people (see Fig. 4), the matching scores differ by, at least, 0.36, as shown in Table 1a.

We also captured images under different lighting conditions (on the second occasion of image capture) to test the robustness of our algorithm. Typical samples are

Fig. 9. Experimental results by the different lighting environments. (a), (c), and (e) normal condition and (b), (d), and (f) adjusted condition.

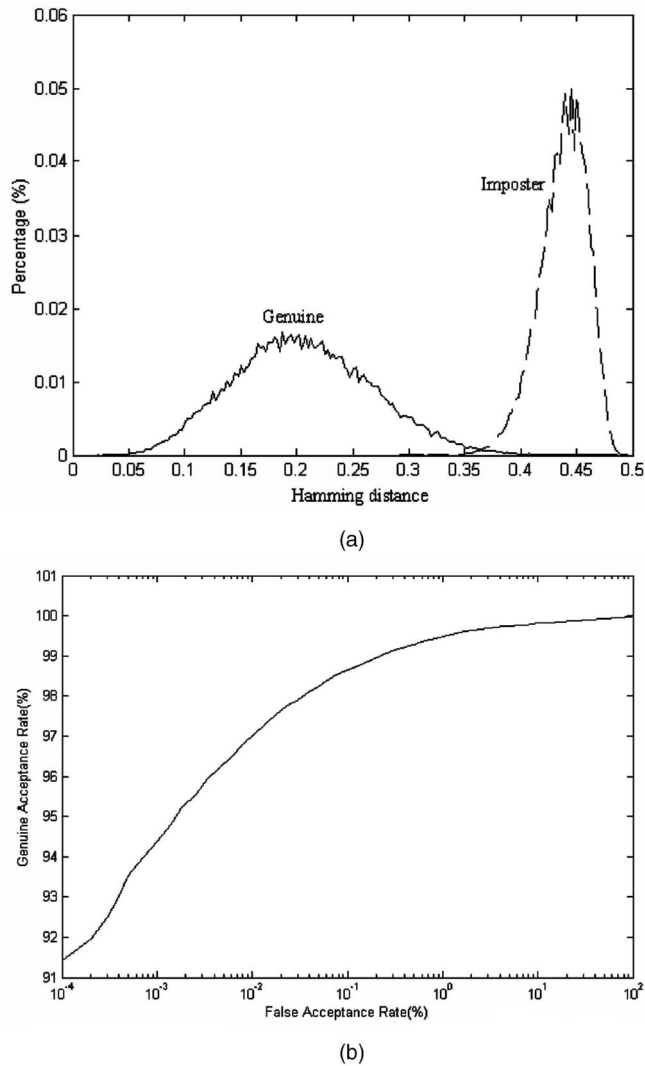


Fig. 10. Verification test results. (a) Genuine and imposter distributions and (b) the receiver operator characteristic curve.

shown in Figs. 9a, 9c, and 9e for normal lighting, and in Figs. 9b, 9d, and 9f for special lighting. Their hamming distances are shown in Table 1c. Although the lighting conditions shown in the second collection of images in Fig. 9 are quite different from the first collection, the proposed system can still easily recognize the same palm. This table gives an insight into the robustness of our system. The overall performance of our system is examined in the experiments described in the next section.

4.2 Verification

To obtain the verification accuracy of our palmprint system, each of the palmprint images was matched with all of the palmprint images in the database. A matching is noted as a correct matching if two palmprint images are from the same palm. The total number of matchings is 30,042,876. None of the hamming distances is zero. The failure to enroll rate is zero. The number of comparisons that have correct matching is 74,086, and the rest are incorrect matchings. The probability distributions for genuine and imposter are estimated by the correct and incorrect matchings, respectively, and are shown in Fig. 10a. Fig. 10b depicts the corresponding Receiver Operating Characteristic (ROC)

curve, which is a plot of genuine acceptance rate against false acceptance rate for all possible operating points. From Fig. 10b, we can see that our system can operate at a 98 percent genuine acceptance rate and a 0.04 percent false acceptance rate, and the corresponding threshold is 0.3425. The system's equal error rate is 0.6 percent. This result is comparable with previous palmprint approaches and other hand-based biometric technologies including hand geometry and fingerprint verification [5], [6], [7], [11], [13], [14], [18], [19].

4.3 Identification

Identification is a process of comparing one image against N images. In the following tests, we setup three registration databases for $N = 50, 100,$ and 200 , which are similar to the number of employees in small to medium sized companies. The first database contains 150 templates from 50 different palms, where each palmprint has three templates. Similarly, for $N = 100$ and 200 , the second and third registration databases have 300 and 600 templates, respectively. We also setup a testing database with 7,152 templates from 386 different palms. None of palmprint images in the testing database are contained in any of the registration

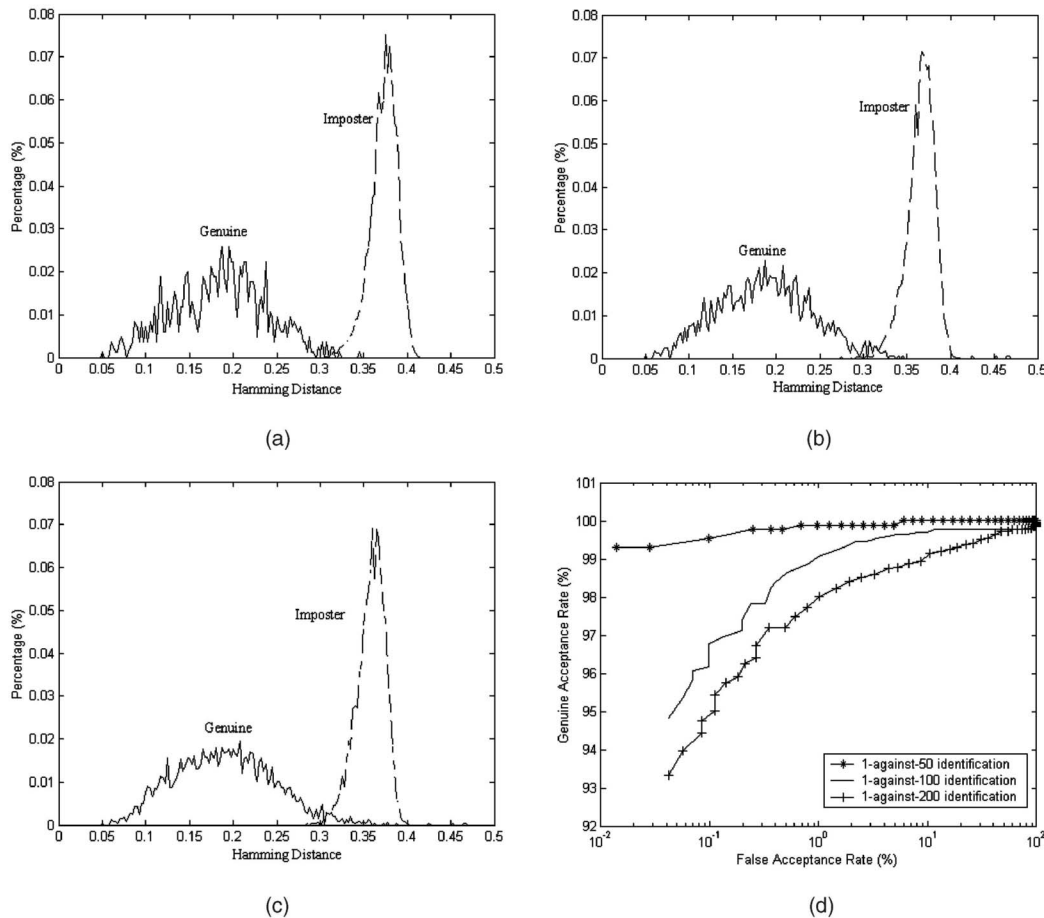


Fig. 11. Identification test results. Genuine and imposter distributions for (a) $N = 50$, (b) $N = 100$, (c) $N = 200$, and (d) their receiver operating characteristic curves.

databases. Each of the palmprint images in the testing database is matched with all of the palmprint images in the registration databases to generate incorrect and correct identification hamming distances. Since a registered palm has three templates in the registration databases, a palmprint image of a registered palm in the testing database is matched with its three templates in the registration databases to produce three correct hamming distances. We take the minimum of these three distances as the correct identification hamming distances. Similarly, a palmprint image in the testing database is compared with all palmprint images in any registration database to produce $3N$ incorrect hamming distances if the testing palmprint does not have any registered images, or $3N-3$ incorrect hamming distances if the palmprint has three registered images. We take the minimum of these distances as the incorrect identification hamming distances. All the imposter identification distributions are generated using the 7,152 incorrect identification hamming distances. The genuine identification distributions are established using the 849, 1,702, and 3,414 correct hamming distances for $N = 50$, 100, and 200, respectively. Figs. 11a, 11b, and 11c illustrate the genuine and imposter distributions and the corresponding ROC curves are shown in Fig. 11d. Comparing the imposter distributions of Figs. 11a, 11b, and 11c, when N increases, the imposter distribution moves to the left. This means that the average of the incorrect identification hamming dis-

tances is reducing. In the experiments, increasing N is equivalent to increasing the number of correct identification hamming distances to establish smoother genuine distributions. Fig. 11d shows that increasing N is equivalent to decreasing the accuracy of the system.

4.4 Speed

The system is implemented using Visual C++ 6.0 on an embedded Intel Pentium III processor (500MHz) PC. The execution time for the preprocessing, feature extraction and matching are 538 ms, 84 ms, and 1.7 ms, respectively. The total execution time is about 0.6 seconds, which is fast enough for real-time verification. For identification, if the database contains images for 100 persons, and each person registers three palmprint images, the total identification time is about 1.1 seconds. In fact, we have not yet optimized the program code, so it is possible that the computation time could be reduced.

5 CONCLUSIONS

We have developed an online palmprint identification system for real-time personal identification by applying a novel CCD camera-based palmprint device to capture the palmprint images. A preprocessing algorithm extracts a central area from a palmprint image for feature extraction. To represent a low-resolution palmprint image and match

different palmprint images, we extend the use of 2D Gabor phase coding to represent a palmprint image using its texture feature, and apply a normalized hamming distance for the matching measurement. Using this representation, the total size of a palmprint feature and its mask is reduced to 384 bytes. In our palmprint database of 7,752 palmprint images from 386 different palms, we can achieve high genuine (98 percent) and low false acceptance (0.04 percent) verification rates, and its equal error rate is 0.6 percent, which is comparable with all other palmprint recognition approaches. This result is also comparable with other hand-based biometrics, such as hand geometry and fingerprint verification [11], [13], [14]. For 1-to-100 identification, our system can operate at a 0.1 percent false acceptance rate and a reasonable 97 percent genuine acceptance rate. The execution time for the whole process, including preprocessing, feature extraction, and final matching, is between 0.6 and 1.1 seconds on a Pentium III processor (500MHz).

In summary, we conclude that our palmprint identification system can achieve good performance in terms of speed and accuracy. For further improvement of the system, we will focus on three issues: 1) to reduce the size of the device for some special applications, 2) to combine the proposed palmprint coding scheme with other texture feature measurements such as texture energy for coarse-level classification to achieve higher performance, and 3) some noisy images with cuts and bruises on the hand have to be collected to test the system.

ACKNOWLEDGMENTS

The authors would like to thank Alex Feng, Brigitta Wan, Rex Fong, and Chun-Sing Wong for their assistance in palmprint image collection. This research is partially supported by the UGC (CRC) fund from the Hong Kong SAR Government, and the central fund from The Hong Kong Polytechnic University. The authors are also most grateful for the constructive advice and comments from the anonymous reviewers.

REFERENCES

- [1] *Biometrics: Personal Identification in Networked Society*. A. Jain, R. Bolle, and S. Pankanti, eds. Boston: Kluwer Academic, 1999.
- [2] D. Zhang, *Automated Biometrics—Technologies and Systems*. Boston: Kluwer Academic, 2000.
- [3] D. Zhang and W. Shu, "Two Novel Characteristics in Palmprint Verification: Datum Point Invariance and Line Feature Matching," *Pattern Recognition*, vol. 32, no. 4, pp. 691-702, 1999.
- [4] N. Duta, A.K. Jain, and K.V. Mardia, "Matching of Palmprint," *Pattern Recognition Letters*, vol. 23, no. 4, pp. 477-485, 2001.
- [5] J. You, W. Li, and D. Zhang, "Hierarchical Palmprint Identification via Multiple Feature Extraction," *Pattern Recognition*, vol. 35, no. 4, pp. 847-859, 2002.
- [6] W. Shu and D. Zhang, "Automated Personal Identification by Palmprint," *Optical Eng.*, vol. 37, no. 8, pp. 2659-2362, 1998.
- [7] W. Shi, G. Rong, Z. Bain, and D. Zhang, "Automatic Palmprint Verification," *Int'l J. Image and Graphics*, vol. 1, no. 1, pp. 135-152, 2001.
- [8] NEC Automatic Palmprint Identification System—<http://www.nectech.com/afis/download/PalmprintDtsht.q.pdf>, 2003.
- [9] P.S. Wu and M. Li, "Pyramid Edge Detection Based on Stack Filter," *Pattern Recognition Letter*, vol. 18, no. 4, pp. 239-248, 1997.
- [10] C.J. Liu and H. Wechsler, "A Shape- and Texture-Based Enhanced Fisher Classifier for Face Recognition," *IEEE Trans. Image Processing*, vol. 10, no. 4, pp. 598-608, 2001.

- [11] A.K. Jain, S. Prabhakar, L. Hong, and S. Pankanti, "Filterbank-Based Fingerprint Matching," *IEEE Trans. Image Processing*, vol. 9, no. 5, pp. 846-859, 2000.
- [12] J.G. Daugman, "High Confidence Visual Recognition of Persons by a Test of Statistical Independence," *IEEE Trans. Pattern Analysis and Machine Intelligence*, vol. 15, no. 11, pp. 1148-1161, Nov. 1993.
- [13] A.K. Jain, L. Hong, and R. Bolle, "On-Line Fingerprint Verification," *IEEE Trans. Pattern Analysis and Machine Intelligence*, vol. 19, no. 4, pp. 302-314, Apr. 1997.
- [14] R. Sanchez-Reillo, C. Sanchez-Avilla, and A. Gonzalez-Marcos, "Biometric Identification through Hand Geometry Measurements," *IEEE Trans. Pattern Analysis and Machine Intelligence*, vol. 22, no. 10, pp. 1168-1171, 2000.
- [15] R.P. Wildes, "Iris Recognition: An Emerging Biometric Technology," *Proc. IEEE*, vol. 85, no. 9, pp. 1348-1363, 1997.
- [16] *Biometric Solutions for Authentication in an e-World*. D. Zhang, ed. Boston: Kluwer Academic, 2002.
- [17] *Advances in Fingerprint Technology*. H.L. Lee and R.E. Gaensslen, eds. second ed., Boca Raton, Fla.: CRC Press, 2001.
- [18] W. Li, D. Zhang, and Z. Xu, "Palmprint Identification by Fourier Transform," *Int'l J. Pattern Recognition and Artificial Intelligence*, vol. 16, no. 4, pp. 417-432, 2002.
- [19] C.C. Han, H.L. Cheng, K.C. Fan, and C.L. Lin, "Personal Authentication Using Palmprint Features," *Pattern Recognition, Special Issue: Biometrics*, vol. 36, no. 2, pp. 371-381, 2003.
- [20] <http://www.primtrakinternational.com/omnitrak.htm>—Primtrak Automatic Palmprint Identification System, 2003.



David Zhang graduated in computer science from Peking University in 1974, and received the MSc and PhD degrees in computer science and engineering from the Harbin Institute of Technology (HIT) in 1983 and 1985, respectively. From 1986 to 1988, he was a postdoctoral fellow at Tsinghua University, and became an associate professor at Academia Sinica, Beijing, China. He received a second PhD degree in electrical and computer engineering at the University of Waterloo, Ontario, Canada, in 1994. Currently, he is a professor at the Hong Kong Polytechnic University. He is the founder and director of two Biometrics Technology Centers supported by the Government of the Hong Kong SAR (UGC/CRC) and the National Nature Scientific Foundation (NSFC) of China, respectively. He is also the founder and editor-in-chief of the *International Journal of Image and Graphics*, book editor of *The Kluwer International Series on Biometrics*, and an associate editor of several international journals, such as *IEEE Transactions on SMC* and *Pattern Recognition*. He is a guest editor of special issues on biometrics in several journals such as *IEEE Transactions on SMC-C* and *Pattern Recognition*, and chairman of the Hong Kong Biometric Authentication Society. His research interests include automated biometrics-based authentication, pattern recognition, biometric technology, and systems. As a principal investigator, he has finished many biometrics projects since 1980. So far, he has published more than 200 papers and seven books, including *Parallel Computer System Designs for Image Processing & Pattern Recognition* (HIT, 1998), *Parallel VLSI Neural System Design* (Springer, 1999), *Automated Biometrics: Technologies and Systems* (Kluwer Academic Publishers, 2000), *Data Management and Internet Computing for Image/Pattern Analysis* (Kluwer Academic Publishers, 2001), *Neural Networks and Systolic Arrays Design* (World Scientific, 2002), and *Biometrics Resolutions for Authentication in an e-World* (Kluwer Academic Publishers, 2002). He is a senior member of the IEEE.



Wai-Kin Kong received the BSc degree in mathematics from Hong Kong Baptist University with first class honors and obtained the MPhil degree from The Hong Kong Polytechnic University. During his study, he received several awards and scholarships from both universities, including scholastic awards and a two year Tuition Scholarship for Research Postgraduate Studies. Currently, he is a research associate in the Department of Computing, The Hong Kong

Polytechnic University. His research interest includes biometric, pattern recognition, image processing, and neural network. He is a member of the IEEE.



Jane You received the BEng degree in electronic engineering from Xi'an Jiaotong University, P.R. China, in 1986, and the PhD degree in computer science from La Trobe University, Australia, in 1992. She was awarded a French Foreign Ministry International Fellowship in 1993. From 1993 to 1995, Dr. You was a lecturer in School of Computing and Information Science, the University of South Australia. From 1996 to 2001, she was with School of Computing

and Information Technology, Griffith University, Australia, where she was a lecturer (1996-1998) and later a senior lecturer (1999-2001). Currently, Dr. You is an academic staff member in the Department of Computing, the Hong Kong Polytechnic University. Her research interests include visual information retrieval, image processing, pattern recognition, multimedia systems, biometrics computing, and data mining. So far, she has more 120 research papers published as journal articles, book chapters, and conference publications in these areas. She is a member of the IEEE.



Michael Wong is a Mphil student in the Department of Computing, The Hong Kong Polytechnic University (PolyU). He received the BA degree in computing in 2001, from PolyU, with first class honors and was awarded The Reuter Foundation Scholarship in 2001. During his study at the Kwai Chung Technical Institutes, he received the CMA & Donors Scholarship Award and The Chiap Hua Cheng's Foundation Scholarship in 1996 and 1997, respectively. He

was one of the group leaders in the Preferred Graduate Development Programme (PGDP 2000), organized by PolyU, and was awarded the Certificate of Achievement for his outstanding leadership and contributions to the PGDP 2000. In his Mphil study, he received a two year Tuition Scholarship for Research Postgraduate Studies awarded by PolyU.

▷ **For more information on this or any other computing topic, please visit our Digital Library at <http://computer.org/publications/dlib>.**